Available online at www.sciencedirect.com

ScienceDirect

journal homepage: www.elsevier.com/locate/he

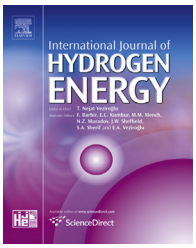

Hydrogen storage in heat welded random CNT network structures

Zeynel Ozturk [a], Cengiz Baykasoglu [b], Alper T. Celebi [c], Mesut Kirca [d], Ata Mugan [d,*], Albert C. To [e,**]

[a] Hitit University, Faculty of Engineering, Department of Chemical Engineering, Cevre Yolu Avenue, 19030 Corum, Turkey

[b] Hitit University, Faculty of Engineering, Department of Mechanical Engineering, Cevre Yolu Avenue, 19030 Corum, Turkey

[c] Southern Methodist University, Lyle School of Engineering, Department of Mechanical Engineering, 3101 Dyer Street Dallas, TX 75205, USA

[d] Istanbul Technical University, Faculty of Mechanical Engineering, Inonu Street, Gumussuyu, 34437 Istanbul, Turkey

[e] University of Pittsburgh, Department of Mechanical Engineering and Materials Science, University of Pittsburgh 508 Benedum Hall, Pennsylvania 15261, USA

ARTICLE INFO

Article history:
Received 5 August 2014
Received in revised form
21 September 2014
Accepted 31 October 2014
Available online 25 November 2014

Keywords:
Random CNT network
Heat welding
Hydrogen storage
Molecular dynamics
Grand canonical Monte Carlo calculation

ABSTRACT

The objective of this study is to investigate hydrogen storage capability of heat welded random carbon nanotube (CNT) network structures. To achieve this objective, different three-dimensional random CNT network structures are generated by using a stochastic algorithm and molecular dynamic simulations. The interaction of CNT networks with hydrogen molecules is then examined via grand canonical Monte Carlo calculations. Hydrogen adsorption capacity of CNT networks having an arbitrarily natured morphology, adjustable porous structure and large surface ratio is investigated. The results show that if cross link density of random CNT networks decreases, hydrogen storage capability of CNT networks increases in terms of the gravimetric capacity. It is observed that random CNT networks could uptake 8.85 wt.% hydrogen at 77 K and this result is very comparable with the results reported in literature where generally ideal ordered nanostructures having no topological irregularities are considered.

Introduction

To solve the problems related to hydrogen storage which are the main barrier in the face of common utilization of hydrogen energy systems, many novel materials such as nonporous and nanostructured carbon materials are investigated [1–3]. Since the discovery of carbon nanotubes (CNTs) by Iijima [4] in 1991, extensive studies have been conducted on

* Corresponding author.
** Corresponding author. Tel.: +1 (412) 624 2052.
E-mail addresses: zeynelozturk@hitit.edu.tr (Z. Ozturk), cengizbaykasoglu@hitit.edu.tr (C. Baykasoglu), acelebi@mail.smu.edu (A.T. Celebi), kircam@itu.edu.tr (M. Kirca), mugan@itu.edu.tr (A. Mugan), albertto@pitt.edu (A.C. To).
http://dx.doi.org/10.1016/j.ijhydene.2014.10.148

their extraordinary properties including hydrogen storage capability. Dillion et al. [5] worked on hydrogen adsorption characteristics of single-walled carbon nanotubes (SWCNT) at 133 K which are prepared by semi-continuous hydrogen arc discharge method. Ye et al. [6] investigated the hydrogen storage of CNTs at a cryogenic temperature of 80 K and under pressures over 12 MPa. Ioannatos et al. [7] studied hydrogen storage behavior of single- and multi-walled CNTs at 77 and 298 K. Yin et al. [8] investigated the gravimetric and volumetric hydrogen storage capacity of SWCNTs at 77 K and 298 K under different pressures. In another study, Liu et al. [9] examined the hydrogen storage behavior of SWCNTs at room temperature. Williams and Erklund [10] presented the results of H-physisorption in a small-diameter SWNT by using classical Monte Carlo simulations and observed the change in the gravimetric density. Zhou et al. [11] studied the hydrogen adsorption behavior of SWCNT arrays by using grand canonical Monte-Carlo (GCMC) simulation. These studies showed that CNTs are not efficient under ambient conditions. In order to increase the hydrogen storage capability at room temperature, the idea of doping CNTs with light alkali metals such as Li or Mg is proposed. Froudakis [12] conducted a comparative study by examining the hydrogen uptake characteristics of alkali-doped SWCNTs and pristine SWCNTs. Chen et al. [13] also investigated the hydrogen adsorption properties by Li and K doped CNTs under ambient conditions. Zhao et al. [14] worked on the hydrogen storage of lithium introduced aromatic carbon materials and it is reported that the poor H_2 binding behavior on undoped aromatic compound alkali metals is improved with Li atom doping. In another study, Ni et al. [15] investigated the hydrogen storage capability of Li-doped charged SWCNTs. A brief literature review about the hydrogen storage of carbon nanotubes can be found in Refs. [2,3,16,17].

Despite the promising properties of CNTs and increment in hydrogen uptake with doping procedure, the amount of storable hydrogen still remains a problematic issue. Therefore, the idea of utilizing novel nanoporous materials having tunable pore structure and large surface area has been targeted to improve the hydrogen storage capacity [18,19]. Consequently, nanoporous materials such as metal-organic frameworks (MOFs) [20–23] and covalent organic frameworks (COFs) [24–27] are considered as ideal structures with high surface/weight ratios and adjustable pore size. Besides these superior properties, the structural stability and lightweightness of carbon based nanomaterials make them a strong candidate for mobile hydrogen storage applications [18,19]. Viculis et al. [28] conducted a study on carbon nanoscrolls (CNSs) and presented the advantages of their potential applications. Mpourmpakis et al. [29] also examined the hydrogen adsorption characteristics in CNSs and pointed out that alkali-doped CNSs are promising materials. Kuc et al. [30] worked on the hydrogen storage nature of fullerene (C_{60}) intercalated graphite (CIG) structures and compared effectiveness of CIGs with those of several selected materials. In a different study, Singh et al. [31] conducted a theoretical study on the hydrogen uptake capacity of carbon-foams and presented the results for different CNT diameters. Furthermore, Dimitrakakis et al. [18] proposed a novel three-dimensional carbon-based nanostructure named as pillared graphene and investigated the improvement on gravimetric and volumetric hydrogen uptake capacity for pristine and Li-doped cases. Wu et al. [32] investigated hydrogen storage behavior of a three dimensional pillared graphene structures by using molecular dynamic simulations. Moreover, recent studies by Tylianakis et al. [33,34] introduced novel carbon-based nanostructures: porous nanotube networks (PNN) and super diamonds to storage hydrogen. Covering both experimental and theoretical approaches, Spyrou et al. [35] presented an extensive literature review about the hydrogen storage capabilities of graphene-based materials and discussed their effectiveness for possible future applications.

In brief, it is concluded that the ordered nanoporous structures dominate the studies on the hydrogen storage in literature. However, the ordered nanostructures are commonly assumed as ideal materials which mean they do not display topological irregularities and highly possible imperfections at junctions such as bond re-arrangements [36,37]. CNT networks generated for experimental studies usually include intricately distributed tubes in space [38]. As a result of that, more realistic structures are needed not only as a hydrogen storage media but also in diverse applications such as advanced composites, nanoelectronics and biotechnology. It has been shown theoretically and experimentally that nanotubes can be merged covalently by using atomic welder during heat treatment or electron irradiation at high temperatures [39]. Hence in our previous works, we proposed a 3-D novel carbon-based nanomaterial called "heat welded random CNT networks" [36,37]. Through molecular dynamics (MD) simulations, we have demonstrated that heat welding is an effective method of forming 3-dimensional continuously welded CNT networks from initially unwelded CNTs [36,40] making this material suitable for experimental studies. The tensile behavior of the CNT networks has also been shown to be good through MD simulations [37]. Underlying the fact that no published work exists in literature presenting the hydrogen storage behavior of random CNT networks, we presented the results about the hydrogen adsorption capacity of CNT network structures having arbitrarily natured morphology, adjustable porous structure and large surface-to-volume ratios. In order to investigate the hydrogen storage capacity of CNT networks, four different network models having different cross-linked densities are simulated by using GCMC simulations under different conditions and the corresponding results are presented.

Modeling and calculations

Atomistic models of the 3-D self-intersected CNT network materials are attained by a cyclic stochastic algorithm that enables generation of randomly distributed CNTs in a user-defined design space while controlling some geometrical parameters such as the CNT length scale, value of cross-linked density, relative angular position of CNT items as well as the length and chirality of CNTs.

According to the generation procedure which is explained thoroughly in Ref. [36], CNT units placed within the network model are not covalently bonded to each other on the cross-link junction regions. Hence, heat welding process is applied

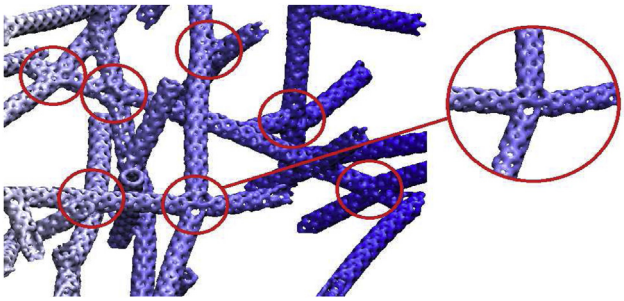

Fig. 1 – Example of junctions throughout a 3-D CNT network.

to the cross-link regions via MD simulations in order to create covalently bonded junctions between intersected CNTs. At this point, different types of junctions (i.e., X, Y and T) are observed to form illustrating the random morphology of the CNT network models. In this regard, several junction regions throughout the network model are shown in Fig. 1.

The heat welding simulations are performed by using LAMMPS (Large-scale Atomic/Molecular Massively Parallel Simulator) that is a publicly-available classical MD code [41]. The Adaptive Intermolecular Reactive Empirical Bond-Order (AIREBO) potential developed by Stuart et al. [42] is used to describe the interactions between carbon atoms. This potential is an extension of the original Brenner's Reactive Empirical Bond-Order (REBO) potential [43] and includes non-bonding atomic interactions. The AIREBO potential enables an investigation on the welding behavior of hydrocarbon molecules by allowing bond breaking and forming mechanisms in covalent bonds [44]. In all network models, CNTs having the chirality of (5,0) and length of 20 nm are used. It is noteworthy at this point that the diameter value of nanotubes is chosen close to the smallest possible theoretical limit for a stable CNT [45] and SWCNTs having approximately a diameter of 0.4 nm are employed in the numerical models just for the sake of minimizing the computational cost. As mentioned in the earlier sections, surface area and pore size are the crucial geometric parameters for enhancing hydrogen storage capacity of nonporous materials. The only topological parameter that is varied in the generation of CNT network structures is the average cross-link density which refers to expected number of CNTs cross-linked with another CNT item and is expected to affect the hydrogen storage properties of CNT network structures. Changing the number of cross-linked CNTs per CNT in the random CNT networks allows us to achieve different porous structures. By this way, four types of CNT network models with 5, 6, 7 and 8 cross-link densities per CNT are generated. Fig. 2 shows the atomistic models of CNT network models having different cross-link densities. More information on the generation of random CNT network models including heat welding process can be found in Refs. [36,37].

Interaction of random CNT network structures with hydrogen is examined by employing GCMC calculations. The Grand Canonical (GC) ensemble is a statistical method that helps calculate the possible locations for the gas molecules inside the models [46]. To this end, Sorption Module of Materials Studio 7.0 software is used for hydrogen storage calculation of the models. The calculations are carried out at three different temperatures: 77 K, 273 K and 298 K. The interaction between hydrogen molecules and carbon atoms and the interaction between hydrogen molecules are modeled by using the Lennard-Jones (LJ) 12-6 potential. Previous computational studies show that Universal Force Field (UFF) can accurately predict diffusion, light gases adsorption and separation in porous materials [11,47–50]; hence, the LJ parameters from the UFF [50] are used to represent the hydrogen molecules and carbon atoms interactions. The hydrogen molecule is represented as a single Van der Waals site (i.e., a united atom model) similar to the works [34,49]. On the other hand, quantum effects are expected to contribute to the absorption process especially at low temperatures [51,52]. In GCMC simulations above 70 K, Feynman–Hibbs (FH) effective potentials are mostly used to estimate the quantum effects which adds a temperature-dependent term to the LJ potential [18,19,49,53]. However, modifications of the potential model in commercial software are often not possible. Hence, the LJ parameters of H_2–H_2 interaction in Refs. [53,54] and Pseudo-FH LJ parameters which are derived by Fischer et al. [49] for $T = 77$ K are used in the LJ potential as only a LJ 12-6 potential is implemented in the software. It is noteworthy that quantum effects on the C–H_2 interaction are not considered in this study. On the other hand, Singh et al. [31] stated that the quantum correction in C–H_2 being less significant than H_2–H_2 correction. Calculations consist of 10 fugacity steps for each temperature in the ranges of 0.1–1 bar and 0.1–100 bars. On the other hand, cubic spline truncation within the cutoff distance of 15.5 Å and spline width of 1 Å are the parameters for

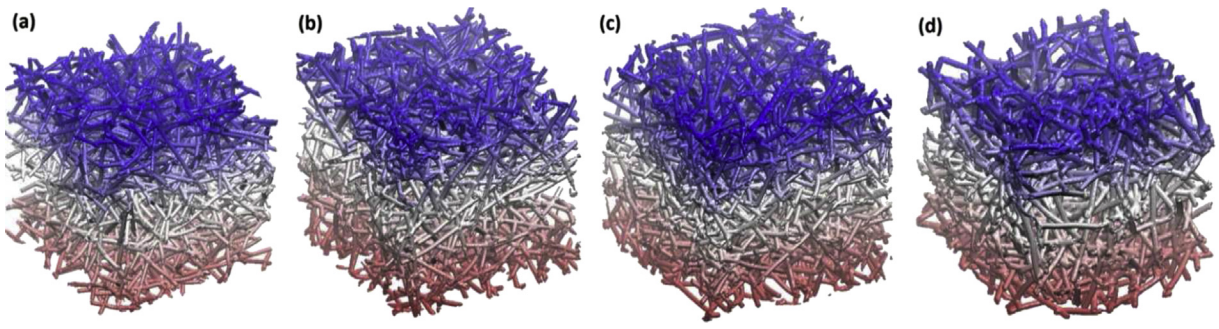

Fig. 2 – CNT network models: (a) 5 cross-link density (model 5), (b) 6 cross-link density (model 6), (c) 7 cross-link density (model 7) and (d) 8 cross-link densities (model 8) per CNT.

atom based vdW summations. Materials Studio 7.0 visualizer is used to create the unit cells from the output file (*.mol) obtained from LAMMPS at the dimensions of 60 × 60 × 60 Å; hence, the unit cell volume (CV) is 216 000 Å^3 for each model. The GCMC simulated cells contain 6172, 7166, 8159 and 9263 carbon atoms for CNT network models having the cross-link densities per CNT as 5, 6, 7 and 8, respectively. It is observed that the dimensions of CNT network specimens have negligible effect on computational results; thus, in order to increase the computational efficiency, optimal unit cell dimension mentioned above is employed in the simulations. Density and unit cell volumes are also calculated by the visualizer and collected from the properties tab for each model. The solvent surface areas are calculated in ultra-fine grid resolution with the grid interval of 0.15 Å. The initial solvent radius is equal to 1.55 Å which is the vdW radii of nitrogen.

Results and discussion

As mentioned above, cross-link density, which is one of the controllable parameters used in the generation process of atomistic models, significantly affects the hydrogen storage capacity of CNT network structures. As the number of CNTs intersected with a CNT unit increases, the cross-link density also increases in parallel. Moreover, the distance between the cross-link locations for the considered CNT unit having constant length decreases along with the increase in cross-link density. Eventually, the mass density of specimen increases. As a result, the density of GCMC simulated cells is respectively calculated as 0.569, 0.661, 0.753 and 0.855 g/cm^3 for cross-link densities per CNT as 5, 6, 7 and 8.

Pore volumes are calculated by using Atom Volumes & Surfaces tool of MS and void fractions (ϕ) are obtained to determine specific pore volumes (v_{pore}) of each CNT model. Void fraction equation which was described by Romanos et al. [55] is used to calculate v_{pore} values. Specific pore volumes for each model are 2.093, 1.418, 1.04 and 0.64 cm^3/g for the Models 5, 6, 7 and 8, respectively. The specific surface areas of each model are used in Kelvin equation to determine pore size distributions. It is found out that the models have mostly micro and meso pores (Fig. 3a). Differential pore volumes show that the Model 5 has the highest value because of the junction density and also the gravimetric density of model. As expected, differential pore values for almost equal pore width range shows different values and the models sorted as Model 5> Model 6> Model 7> Model 8 similar to cumulative pore volume values at different pore widths shown in Fig. 3b.

While the hydrogen is loaded into models, namely it is adsorbed, the interactions between the hydrogen molecules and CNTs are vdW interactions and the adsorption is also called physical adsorption or physisorption. Representation of the locations of hydrogen molecules around the CNTs is shown in Fig. 4. The distance between the closest hydrogen molecule and CNT walls is approximately 3 Å. According to force field potentials (i.e., 12-6 potential), the distances between hydrogen molecules and CNT wall can be calculated. Interaction potentials increase abnormally at approximately 2.8 Å distance which means that Van der Waals interactions do not exist at that region. Some selected hydrogen molecules were 3.387, 3.269, 3.074, 2.907 and 2.867 Å far from CNT walls which are shown in Fig. 4.

In the following, the vdW, solvent and accessible solvent surface area of network models having the cross-link densities per CNT of 5, 6, 7 and 8 are calculated. Accessible solvent surface areas of CNT network model having 6 cross-link densities are shown in Fig. 5a where the blue layer is the outer surface and the gray layer is the inner surface. The vdW surfaces are the layer that covers the outer side of molecules in the distance of vdW radii which is 1.7 Å for carbon atoms which is shown in Fig. 5b as the blue layer. The accessible solvent and solvent surface areas are calculated by considering the uptake of nitrogen gas which has the vdW radii of 1.55 Å. This is chosen because the surface area and adsorption characteristics are commonly measured by the nitrogen gas in experiments. Considering the solvent surface and accessible solvent surface calculations by using the nitrogen with the

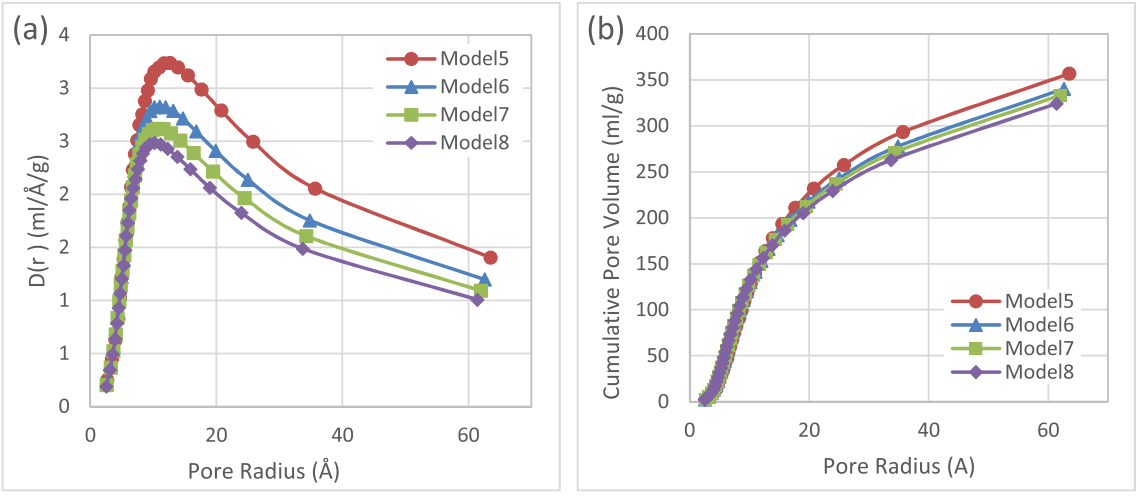

Fig. 3 – Pore size distribution curves of models; (a) differential pore volume and (b) cumulative pore volumes versus pore radius.

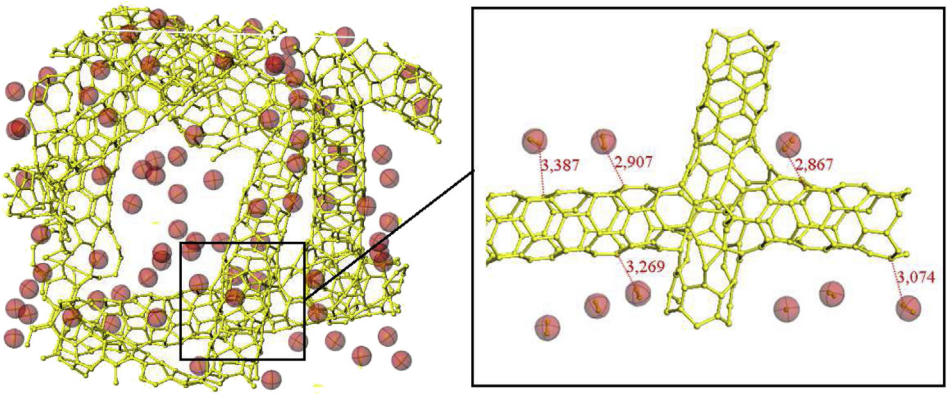

Fig. 4 – Interactions between hydrogen molecules and CNT walls.

vdW radii of 1.55 Å, that are represented in Fig. 5b with yellow dotted layer, no reasonable difference exists between the solvent and accessible solvent surface areas. It is also found out that there are small vdW surfaces on the inner sides of CNTs in all models. This is the reason why there are differences between vdW surfaces and solvent/accessible solvent surface areas. In other words, solvent/accessible solvent surfaces are smaller than the vdW surface areas; thus, the solvents as well as the hydrogen could not diffuse into the spaces inside the carbon nanotubes.

It can be seen in Table 1 that when the surface areas are calculated in the unit of $Å^2$/per cell, the highest values are observed for the cross-link density of 8 for the vdW, solvent and accessible solvent surface areas. On the other hand, the comparison gets unclear when the units of $Å^2$/per cell are used because gravimetric densities are also important and should be evaluated. It is observed in Table 1 that the model having the cross-link density of 5 has the highest accessible solvent surface area and thus relatively higher hydrogen uptake. Note that the gravimetric surface area of the model having the cross-link density of 5 given in Table 1 is very similar to the model constructed by Tylianakis et al. [34].

The potential places in which hydrogen could be stored inside the models are also simulated and shown in Fig. 6a for the model having the cross-link density of 6. The potential places are different for each model, and it is observed that they are getting smaller with the effects of pressure and temperature. In physical adsorption, the potential places for gas adsorption reduce with increasing pressure and decreasing temperature as described in the presentation of GCMC ensemble by Yao et al. [56]. Hydrogen molecules inside the model having the cross-link density of 6 are also shown in Fig. 6b where the red ellipsoids are hydrogen molecules while the green structure is CNTs.

Total and excess hydrogen uptake capacities of models are calculated and corresponding results are given in separate graphs for different temperatures (e.g., see Ref. [Figs. 7–9]). It can be observed in Fig. 7 that gas adsorptions show Type I isotherms due to existence of micro and meso pores in CNT networks (i.e., Fig. 3). On the other hand, quantum correction decreases the total uptake in real adsorption systems at low

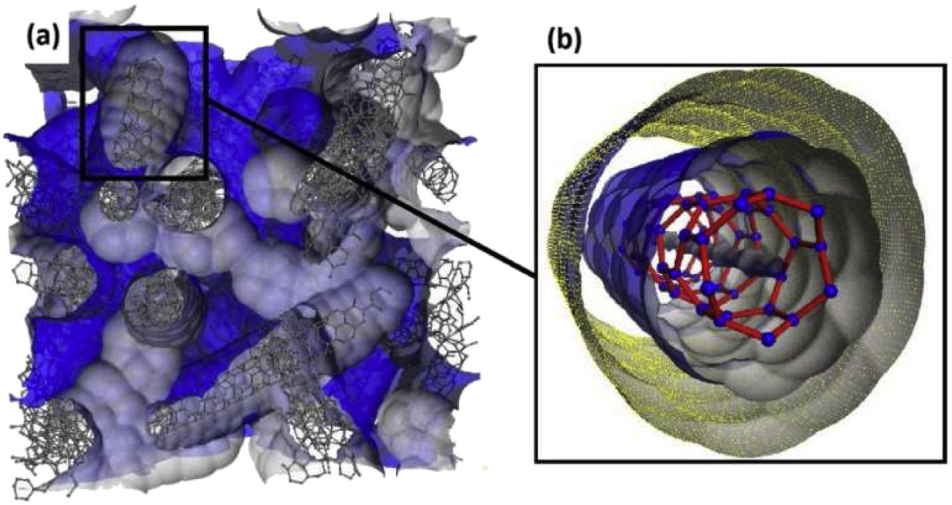

Fig. 5 – Surface area simulations representation: (a) general view, (b) solvent-accessible surfaces in the yellow dotted blue layer and vdW surfaces in blue. (For interpretation of the references to color in this figure legend, the reader is referred to the web version of this article.)

Table 1 – The vdW, solvent and accessible solvent surface areas for different cross-link densities and in terms of the units of Å²/per cell and m²/g.

Cross-link density	vdW surface area		Solvent surface area		Accessible solvent surface area	
	(Å²/per cell)	m²/g	(Å²/per cell)	m²/g	(Å²/per cell)	m²/g
5	33108.47	2689.57	30803.30	2502.31	30798.14	2501.89
6	38061.51	2663.06	31481.00	2202.63	31477.47	2202.39
7	41683.15	2561.50	33068.26	2032.10	33062.15	2031.72
8	46110.71	2495.86	35257.81	1908.42	35251.57	1908.08

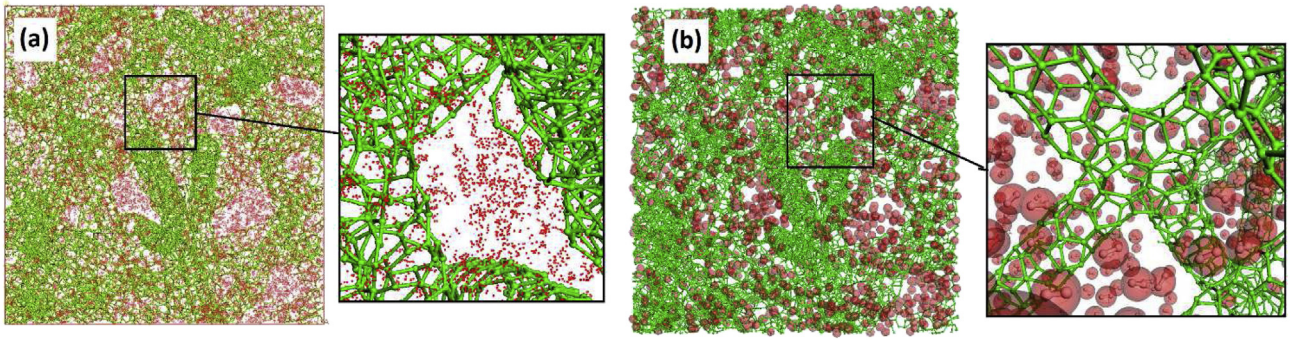

Fig. 6 – (a) Potential places for the hydrogen adsorption inside the CNT model are represented in red dots and (b) the stored hydrogen in the model 6 is shown by red ellipsoids. (For interpretation of the references to color in this figure legend, the reader is referred to the web version of this article.)

temperatures. It is observed that quantum correction especially affect the results at 77 K and the differences between corrected and un-corrected results are found as approximately 5% which is in agreement with other reports [53]. Hydrogen storage properties over 100 bars are not studied because the promising pressure for the hydrogen is limited by 150 bars; in addition, many researchers worked up to the maximum pressure of 100 bars. This limitation could help us to easily make comparison of the hydrogen storage properties. Measurements at 77 K are important because it is the lowest temperature that can be reached easily by using cryogenic nitrogen. At the same time, for the considered materials valuable uptake capacities can be reached by physisorption at low temperatures. The ice melting point of 273 K and the room temperature of 298 K are set as the other temperatures. The hydrogen storage property of models decreases by increasing density of the models as can be seen in Figs. 7–9. It is found that the model having the cross-link density of 5 has the highest hydrogen storage capacity for each temperature as expected from high accessible solvent surface area values (i.e., see Figs. 7–9). Under the pressure range of 0.1–100 bars, the model having the cross-link density of 5 could uptake 8.85 wt.%. On the other hand, uptake capacities are calculated 7.23, 6.20 and 5.01 wt.% for the Models 6, 7 and 8, respectively. When the results of models having the cross-links of 5 and 8 are compared, 43.39% decrease in hydrogen uptake are found

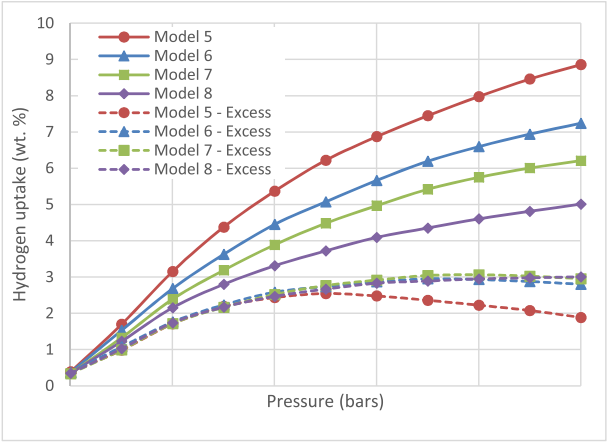

Fig. 7 – Total and excess hydrogen storage properties of models at 77 K.

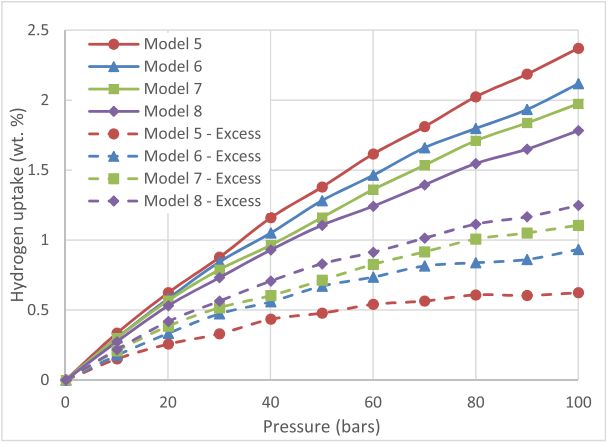

Fig. 8 – Total and excess hydrogen storage properties of models at 273 K.

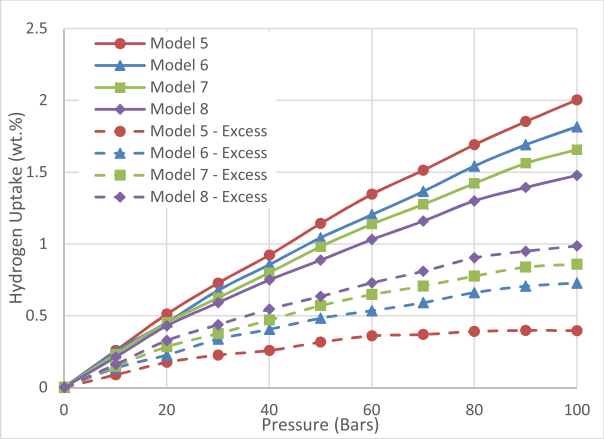

Fig. 9 – Total and excess hydrogen storage properties of models at 298 K.

while the density increases 50.26% at 77 K and under the pressure of 100 bars. In parallel, the uptake capacity at 77 K and under the maximum pressure of 1 bar are 3.34, 2.97, 2.92 and 2.84 wt.% for the Models 5, 6, 7 and 8, respectively.

In the range of 0.1–100 bars at 77 K, hydrogen adsorption shows curvy trend as commonly encountered in literature. Nonlinear ascending behavior of hydrogen uptake with rising pressure represents existing of the micro porosity and effect of fluid–fluid interactions. In the other word, high pressures enforce hydrogen molecules to place together after mono and multilayer adsorption on the CNT walls at 77 K. Another specific parameter can be used to compare hydrogen storage capacity of adsorbent is excess adsorption. Excess adsorption curves differ from the total uptake. Excess adsorption refers the amount of hydrogen adsorbed on the surface of adsorbent. In the present work minimum excess amount is observed in the model having 5 cross-links while it has the maximum total uptake at 77 K and under 100 bars. The excess hydrogen amounts are 1.88, 2.80, 2.98 and 3.00 wt.% for the models having the cross-links of 5, 6, 7 and 8, respectively.

Hydrogen storage capacities of the models at 273 and 298 K decrease as expected in comparison with that of 77 K. The maximum hydrogen uptake at 273 K is found about 2.37 wt.% in the model having 5 cross-links. For the same conditions, the total uptakes are 2.11, 1.97 and 1.78 wt.% for the models having the cross-links of 6, 7 and 8, respectively. Overall, the hydrogen absorption value of the model having 8 cross-links is about 24.89% smaller than that of the network with 5 cross-links. At -room temperature, the maximum uptake is found about 2.09 wt.% for the model having 5 cross-links. The models having the cross-links of 6, 7 and 8 uptake respectively 1.81, 1.65 and 1.47 wt.% hydrogen at room temperature and under 100 bars. Excess uptake values are respectively shown in Figs. 8 and 9 for the temperatures of 273 and 298 K. Uptake at low pressures (i.e.,1 bar) for the temperatures of 273 and 298 K are too small against the low temperatures and high pressures. The maximum uptake at 273 K and 1 bar are 0.039, 0.034, 0.030 and 0.027 wt.% and the values decrease to 0.025, 0.024, 0.023 and 0.021 wt.% at 298 K and 1 bar for the Models 5, 6, 7 and 8, respectively.

Table 2 presents the hydrogen storage values of several selected carbon-based nanostructures in literature and found in our simulations. These results are better than carbon based structures that generally do not overpass 5 wt.%. In addition, these results are very comparable with the results reported in literature where generally ideal ordered nanostructures having no topological irregularities are considered. Hence, proposed random CNT networks having adjustable porous structure and large surface ratio are potential candidates for future hydrogen storage applications.

Conclusion

In this study, hydrogen storage capacity in heat welded random CNT network structures is examined by using the GCMC calculations. The proposed novel CNT network structure enables to obtain arbitrarily natured morphology, variable pore and large surface sizes; thus, it provides more

Table 2 – Summary of hydrogen uptake capacities of similar adsorbents in different conditions.

Adsorbent	Temperature (K)	Pressure (bar)	H_2 uptake (wt.%)	Reference
Random CNT	77	100	**8.85**	Present work (Model 5)
Random CNT	77	1	**3.34**	Present work (Model 5)
Random CNT	273	100	**2.37**	Present work (Model 5)
Random CNT	298	100	**2.00**	Present work (Model 5)
SWCNT	300	10	4.20	Liu et al. [9]
Pillared graphene	77	100	7.2	Dimitrakakis et al. [18]
Pillared graphene	300	100	1.4	Dimitrakakis et al. [18]
Porous nanotube network	77	100	~5.8–23.6	Tylianakis et al. [33]
Diamond-like super structures of CNTs	77	100	~9.5–24.1	Tylianakis et al. [34]
Diamond-like super structures of CNTs	300	100	~2.0–8.35	Tylianakis et al. [34]
SWCNT	80	100	11.00	Darkim et al. [57]
MWCNT	298	100	0.68	Zhu et al. [58]
SWCNT	77	1	2.37	Nishimiya et al. [59]
SWCNT	77	100	2.75–3.60	Yuca and Karatepe [60]
SWCNT	298	97	0.32	Kumar et al. [61]
MWCNT	298	100	0.2	Yang et al. [62]
MWCNT	77	1	0.21	Yang et al. [62]

flexibility to control the geometric features that affect the hydrogen storage capacity. As a result of GCMC calculations, it is shown that hydrogen uptake capacity of models reduced by increasing the cross-link density; in other words, while the number of junctions per CNT unit within the network is increasing, hydrogen storage ability decreases because the amount of potential CNT surfaces where hydrogen molecules could be adsorbed is getting smaller. In conclusion, the best model for the hydrogen storage at the temperatures of 77, 273 and 298 K and in the ranges of 0.1–1 bar and 0.1–100 bars is determined to be the model having 5 cross-links. The main handicap for the hydrogen storage in the constructed models is the diameter of CNTs. The proposed diameter value is close to the theoretical limit for a stable CNT and the tubes having such a small diameter allow no adsorption inside the tubes or limit the diffusion to inner sides of the tubes. In future, effects of nanotube diameter, length and chirality on hydrogen storage capacity of random network model will be studied. In addition, Li, Pt and other metal doped random CNT structures will also be considered to enhance hydrogen adsorption at room temperature.

Acknowledgment

This research is supported in part by Hitit University Research Project under the grant number MUH19007.14.002.

REFERENCES

[1] Thomas KM. Hydrogen adsorption and storage on porous materials. Catal Today 2007;120(3):389–98.
[2] Yürüm Y, Taralp A, Veziroglu TN. Storage of hydrogen in nanostructured carbon materials. Int J Hydrogen Energy 2009;34(9):3784–98.
[3] Oriňáková R, Oriňák A. Recent applications of carbon nanotubes in hydrogen production and storage. Fuel 2011;90(11):3123–40.
[4] Iijima S. Helical microtubules of graphitic carbon. Nature 1991;354:56–8.
[5] Dillon AC, Jones KM, Bekkedahl TA, Kiang CH, Bethune DS, Heben MJ. Storage of hydrogen in single-walled carbon nanotubes. Nature 1997;386(6623):377–9.
[6] Ye Y, Ahn CC, Witham C, Fultz B, Liu J, Rinzler AG, et al. Storage of hydrogen in single-walled carbon nanotubes. Appl Phys Lett 1999;74(16):2307–9.
[7] Ioannatos GE, Verykios XE. H_2 storage on single-and multi-walled carbon nanotubes. Int J Hydrogen Energy 2010;35(2):622–8.
[8] Yin YF, Mays T, McEnaney B. Molecular simulations of hydrogen storage in carbon nanotube arrays. Langmuir 2000;16:10521–7.
[9] Liu C, Fan YY, Liu M, Cong HT, Cheng HM, Dresselhaus MS. Hydrogen storage in single-walled carbon nanotubes at room temperature. Science 1999;286(5442):1127–9.
[10] Williams KA, Erklund PC. Monte Carlo simulations of H physisorption in finite-diameter 2 carbon nanotube ropes. Chem Phys Lett 2000;320:352–8.
[11] Zhou S, Liu X, Yang K, Zou H. Study of H_2 physical adsorption in single-walled carbon nanotube array. AIP Adv 2013;3:082119.
[12] Froudakis GE. Why alkali-metal-doped carbon nanotubes possess high hydrogen uptake. Nano Lett 2001;1(10):531–3.
[13] Chen P, Wu X, Lin J, Tan KL. High H_2 uptake by alkali-doped carbon nanotubes under ambient pressure and moderate temperatures. Science 1999;285(5424):91–3.
[14] Zhao YL, Zhang RQ, Wang RS. The role of lithium in hydrogen storage in aromatic carbon materials. Chem Phys Lett 2004;396:62–7.
[15] Ni M, Huang L, Guo L, Zeng Z. Hydrogen storage in Li-doped charged single-walled carbon nanotubes. Int J Hydrogen Energy 2010;35(8):3546–9.
[16] Darkrim FL, Malbrunot P, Tartaglia GP. Review of hydrogen storage by adsorption in carbon nanotubes. Int J Hydrogen Energy 2002;27(2):193–202.
[17] Ströbel R, Garche J, Moseley PT, Jörissen L, Wolf G. Hydrogen storage by carbon materials. J Power Sources 2006;159(2):781–801.
[18] Dimitrakakis GK, Tylianakis E, Froudakis GE. Pillared graphene: a new 3-D network nanostructure for enhanced hydrogen storage. Nano Lett 2008;8(10):3166–70.
[19] Tylianakis E, Psofogiannakis, Froudakis GE. Li-doped pillared graphene oxide: a graphene-based nanostructured material for hydrogen storage. J Phys Chem Lett 2010;1:2459–64.
[20] Rosi NL, Eckert J, Eddaoudi M, Vodak T, Kim J, O'Keeffe M, et al. Hydrogen storage in microporous metal-organic frameworks. Science 2003;300:1127–9.
[21] Rowsell JLC, Yaghi OM. Strategies for hydrogen storage in metal–organic frameworks. Angew Chem Int Ed 2005;44:4670–9.
[22] Rowsell JLC, Millward AR, Park KS, Yaghi OM. Hydrogen sorption in functionalized metal–organic frameworks. J Am Chem Soc 2004;126:5666–7.
[23] Volkova EI, Vakhrushev AV, Suyetin M. Improved design of metal-organic frameworks for efficient hydrogen storage at ambient temperature: a multiscale theoretical investigation. Int J Hydrogen Energy 2014;39(16):8347–50.
[24] El-Kaderi HM, Hunt JR, Mendoza-Cortés JL, Côté AP, Taylor RE, O'Keeffe M, et al. Designed synthesis of 3D covalent organic frameworks. Science 2007;316:268–72.
[25] Garberoglio G. Computer simulation of the adsorption of light gases in covalent organic frameworks. Langmuir 2007;23:12154–8.
[26] Han SS, Furukawa H, Yaghi OM, Goddard III WA. Covalent organic frameworks as exceptional hydrogen storage materials. J Am Chem Soc 2008;130:11580–1.
[27] Li F, Zhao J, Johansson B, Sun L. Improving hydrogen storage properties of covalent organic frameworks by substitutional doping. Int J Hydrogen Energy 2010;35(1):266–71.
[28] Viculis LM, Mack JJ, Kaner RB. A chemical route to carbon nanoscrolls. Science 2003;299:1361.
[29] Mpourmpakis G, Tylianakis E, Froudakis GE. Carbon nanoscrolls: a promising material for hydrogen storage. Nano Lett 2007;7(7):1893–7.
[30] Kuc A, Zhechkov L, Patchkovskii S, Seifert G, Heine T. Hydrogen sieving and storage in fullerene intercalated graphite. Nano Lett 2007;7(1):1–5.
[31] Singh AK, Lu J, Aga RS, Yakobson BI. Hydrogen storage capacity of carbon-foams grand canonical monte carlo simulations. J Phys Chem 2011;115:2476–82.
[32] Wu CD, Fang TH, Lo JY. Effects of pressure, temperature, and geometric structure of pillared graphene on hydrogen storage capacity. Int J Hydrogen Energy 2012;37(19):14211–6.
[33] Tylianakis E, Dimitrakakis GK, Martin-Martinez FJ, Melchor S, Dobado JA, Klontzas E, et al. Porous nanotube network: a novel 3-D nanostructured material with enhanced hydrogen storage capacity. Chem Commun 2011;47:2303–5.

[34] Tylianakis E, Dimitrakakis GK, Melchor S, Dobado JA, Froudakis GE. Designing novel nanoporous architectures of carbon nanotubes for hydrogen storage. Int J Hydrogen Energy 2014;39:9825–9.
[35] Spyrou K, Gournis K, Rudolf P. Hydrogen storage in graphene-based materials efforts towards enhanced hydrogen absorption. ECS J Solid State Sci Technol 2013;2(10):3160–9.
[36] Kirca M, Yang X, To AC. A stochastic algorithm for modeling heat welded random carbon nanotube network. Comput Methods Appl Mech Eng 2013;259:1–9.
[37] Celebi AT, Kirca M, Baykasoglu C, Mugan A, To AC. Tensile behavior of heat welded CNT network structures. Comp Mater Sci 2014;88:14–21.
[38] Assfour B, Leoni S, Seifert G, Baburin IA. Packings of carbon nanotubes–new materials for hydrogen storage. Adv Mat 2011;23(10):1237–41.
[39] Romo-Herrera JM, Terrones M, Terrones H, Dag S, Meunier V. Covalent 2D and 3D networks from 1D nanostructures: designing new materials. Nano Lett 2007;7(3):570–6.
[40] Yang X, Han Z, Li Y, Chen D, Zhang P, To AC. Heat welding of non-orthogonal x-junction of single-walled carbon nanotubes. Phys E 2012;46:30–2.
[41] Plimpton S. Fast parallel algorithms for short-range molecular-dynamics. J Comput Phys 1995;117:1–19.
[42] Stuart SJ, Tutein AB, Harrison JA. A reactive potential for hydrocarbons with intermolecular interactions. J Chem Phys 2000;112:6472–86.
[43] Brenner DW, Shenderova OA, Harrison JA, Stuart SJ, Ni B, Sinnott SB. A second-generation reactive empirical bond order (REBO) potential energy expression for hydrocarbons. Condens. Matter 2002;14:783–802.
[44] Faria B, Silvestre N, Canongia Lopes JN. Tension–twisting dependent kinematics of chiral CNTs. Compos Sci Technol 2013;74:211–20.
[45] Zhao X, Liu Y, Inoue S, Suzuki T, Jones R, Ando Y. Smallest carbon nanotube is 3 Å in diameter. Phys Rev Lett 2004;92(12):125502.
[46] Gibbs WJ. Elementary principles in statistical mechanics. New York, London: Charles Scribner's Sons; 1902. Edward Arnold.
[47] Lee TB, Jung DH, Kim D, Kim J, Choi K, Choi SH. Molecular dynamics simulation study on the hydrogen adsorption and diffusion in non-interpenetrating and interpenetrating IRMOFs. Catal Today 2009;146(1):216–22.
[48] Poirier E. Ultimate H_2 and CH_4 adsorption in slit-like carbon nanopores at 298 K: a molecular dynamics study. RSC Adv 2014;4(44):22848–55.
[49] Fischer M, Hoffmann F, Fröba M. Preferred hydrogen adsorption sites in various MOFs-a comparative computational study. ChemPhysChem 2009;10(15):2647–57.
[50] Rappe AK, Casewit CJ, Colwell KS, Goddard WAI, Skiff WM. UFF, a full periodic table force field for molecular mechanics and molecular dynamics simulations. J Am Chem Soc 1992;114:10024–35.
[51] Wang Q, Johnson JK. Computer simulations of hydrogen adsorption on graphite nanofibers. J Phys Chem B 1999;103:277–81.
[52] Kumar AVA, Jobic H, Bhatia SK. Quantum effect induced kinetic molecular sieving of hydrogen and deuterium in microporous materials. Adsorption 2007;13:501–8.
[53] Kuchta B, Firlej L, Pfeifer P, Wexler C. Numerical estimation of hydrogen storage limits in carbon-based nanospaces. Carbon 2010;48(1):223–31.
[54] Buch V. Path integral simulations of mixed para-D_2 and ortho-D_2 clusters: the orientational effects. J Chem Phys 1994;100:7610–29.
[55] Romanos J, Beckner M, Rash T, Firlej L, Kuchta B, Yu P, et al. Nanospace engineering of KOH activated carbon. Nanotechnology 2012;23(1):015401.
[56] Yao J, Greenkorn RA, Chao KC. Monte Carlo simulation of the grand canonical ensemble. Mol Phys An Int J A T interface between Chem Phys 1982;46:587–94.
[57] Darkrim FL, Levesque D. High adsorptive property of opened carbon nanotubes at 77 K. J Phys Chem B 2000;104:6773.
[58] Zhu H, Cao A, Li X, Xu C, Mao Z, Ruan D, et al. Hydrogen adsorption in bundles of well-aligned carbon nanotubes at room temperature. Appl Surf Sci 2001;178:50.
[59] Nishimiya N, Ishigaki K, Takikawa H, Ikeda M, Hibi Y, Sakakibara T, et al. Hydrogen sorption by single-walled carbon nanotubes prepared by a torch arc method. J Alloys Compd 2002;339:275.
[60] Yuca N, Karatepe N. Hydrogen storage in single-walled carbon nanotubes purified by microwave digestion method. world academy of Science. Eng Technol 2011;5:513–8.
[61] Kumar KV, Salih A, Lu L, Müller EA, Rodríguez-Reinoso F. Molecular simulation of hydrogen physisorption and chemisorption in nanoporous carbon structures. Adsorpt Sci Tech 2011;29(8):799–818.
[62] Yang SJ, Cho JH, Nahm KS, Park CR. Enhanced hydrogen storage capacity of Pt-loaded CNT@ MOF-5 hybrid composites. Int J Hydrogen Energy 2010;35(23):13062–7.